Available online at www.sciencedirect.com
SCIENCE DIRECT
Catalysis Today 107–108 (2005) 417–425
CATALYSIS TODAY
www.elsevier.com/locate/cattod

Study of Ce-Zr-Co fluorite-type oxide as catalysts for hydrogen production by steam reforming of bioethanol

Julio César Vargas [a,b,*], Suzanne Libs [b], Anne-Cécile Roger [b], Alain Kiennemann [b]

[a] *Departamento de Ingeniería Química, Universidad Nacional de Colombia, Ciudad Universitaria, Avenida Carrera 30 N° 45-03, Edificio 453, Bogotá D.C., Colombia*
[b] *Laboratoire des Matériaux, Surfaces et Procédés pour la Catalyse LMSPC, UMR CNRS 7515 ECPM, Université Louis Pasteur, 25 rue Becquerel, 67087 Strasbourg Cedex 2, France*

Available online 24 August 2005

Abstract

Bioethanol, obtained by biomass fermentation, could be an important hydrogen supplier as a renewable source. The development of active, selective and stable catalysts for bioethanol steam reforming is a key point.

In this work, a fluorite type Ce-Zr-Co oxide, $Ce_2Zr_{1.5}Co_{0.5}O_{8-\delta}$, is studied for hydrogen production by steam reforming of ethanol/water mixture and bioethanol solution. The catalyst is characterized before and after catalytic test by X-ray diffraction (XRD), scanning electron microscopy (SEM) and transmission electron microscopy with energy dispersive X-ray spectroscopy (TEM-EDX). The preparation method based on propionate polymerization in solution ensures the insertion of cobalt in the mixed oxide lattice and provides high micro-homogeneity at nanoscale level.

The reduction procedure to activate the catalysts is controlled by thermo programmed reduction (TPR).

The partially reduced Ce-Zr-Co oxide catalyst presents high ethanol conversion and high hydrogen selectivity. Superior alcohols (fusel oils) arising from the fermentation process do not influence the catalytic behavior compared to a model ethanol/water mixture.

Decreasing activity is related to the formation of carbon filaments, evidenced by thermo programmed oxidation (TPO) measurements and transmission electron microscopy.

Keywords: Hydrogen; Bioethanol; Steam reforming; Fluorite; Ce-Zr-Co

1. Introduction

As a consequence of the more and more stringent environmental standards and of the decline of the fossil fuels reserves, the growing energy demand has to be supplied from renewable and sustainable, efficient and cost-effective, convenient and safe energy systems [1]. Bioethanol, produced by biomass fermentation, has a great potential for the production of hydrogen and energy.

The design of an active, selective and stable catalytic system for the steam reforming of ethanol is one of the key points. The catalyst has to optimize the hydrogen production and to discourage the by-products formation.

Various catalysts are studied for the reaction of ethanol steam reforming: oxides [2], oxide-supported transition metals [3–7] or noble metals [8,9]. Among the reported catalysts, the cobalt-based systems seem to be the most promising. They are generally prepared by impregnation of various supports [4,5,7]. The catalysts deactivation is attributed to carbon formation and deposition [3,5,6]. The metal-oxide interaction, which appears as essential for the stability, and the understanding of the active phase are reported only recently [5,10].

The studies of the ethanol steam reforming are not systematically carried out under realistic reaction conditions as regards the ethanol/water ratio as well as the ethanol composition.

* Corresponding author.
E-mail addresses: jcvargass@unal.edu.co, vargasjc@ecpm.u-strasbg.fr (J.C. Vargas).

0920-5861/$ – see front matter © 2005 Elsevier B.V. All rights reserved.
doi:10.1016/j.cattod.2005.07.118

First, the ethanol/water molar ratio varies from 1:23 to 1:2.5 [2,5,6,10,11]. The 1:23 ratio corresponds to a 10% (w/v) solution, which is the typical concentration of bioethanol solution after fermentation. The 1:2.5 ratio is below the stoichiometry of the reaction. There is in fact a compromise to find between the cost of distillation to concentrate the bioethanol solution before the reforming reaction to increase the H_2 production per volume of initial solution, and the cost of vaporization of the excess of water (for ethanol/water ratios lower than the stoichiometric value of 1:3) in the reforming reaction. Furthermore, it has to be kept in mind that an excess of water with respect to the stoichiometry has a beneficial effect to avoid or reduce the carbon deposition on the catalyst.

Second, the ''bioethanol'' solution often reported in the literature is in fact a mixture of water and ethanol, the real composition of bioethanol obtained by fermentation and simple distillation (water, methanol, ethanol, and the denominated fusel oil composed by *n*-propyl, *n*-butyl, *sec*-butyl, isobutyl and *n*-amyl and isoamyl alcohols), being not taken into account [12].

In previous works, we demonstrated the efficiency of cobalt-doped Ce-Zr fluorite oxide catalysts for the production of hydrogen from ethanol steam reforming (ethanol/water ratio of 1:6). It was shown that the initial integration of cobalt in the oxide lattice strongly increases the catalysts stability under test when compared to impregnated catalysts [13]. Among the $Ce_2Zr_{2(1-x)}Co_{2x}O_{8-\delta}$ series (with $0 \leq x \leq 0.625$), the catalyst of formula $Ce_2Zr_{1.5}Co_{0.5}O_{8-\delta}$ was shown to be the most cobalt-loaded mixed oxide in which no cobalt oxide rejection was observed [14].

In this work, we present the catalytic behavior of $Ce_2Zr_{1.5}Co_{0.5}O_{8-\delta}$ for the hydrogen production by steam reforming of ethanol: real bioethanol solution (ethanol/water ratio of 1:5.95) obtained by sugar cane molasses fermentation and subsequent simple distillation, and ethanol/water mixture (ethanol/water ratio of 1:6). The deactivation under test are compared. The catalyst evolution with time on stream is discussed to explain the deactivation.

2. Experimental

2.1. Production of bioethanol

The synthesis of bioethanol was carried out by discontinuous simple fermentation of sugarcane molasses with *Saccharomyces cerevisiae* as yeast.

First, sugarcane molasses were diluted with water until a density of 1.078 was obtained. The pH of the solution was adjusted to 4.45 with H_2SO_4 solution at 98%.The substrate was heated at 30 °C under stirring. At this temperature, the *S. cerevisiae* yeast culture was added, the stirring was stopped, and the batch reactor was closed. Attention was paid to the temperature, which has to be maintained around 30 °C, and in any case lower than 35 °C. The fermentation reaction proceeded for 72 h. After fermentation the pH was adjusted to 6.5 with sodium hydroxide.

The neutral solution was submitted to a simple distillation at 60 °C to eliminate most byproducts and concentrate the solution in ethanol. The composition of the such obtained bioethanol solution was studied by gas chromatography. The solution is mainly composed of water and ethanol, and contains traces of methanol, *n*-propanol, *n*-butanol and *iso*-amilic alcohol. The molar ratio ethanol/water is 1:5.95. The relative density is 0.952 at 20 °C, and corresponds to 30–31% (w/v) of ethanol.

2.2. Preparation and characterization of catalysts

The fluorite oxide $Ce_2Zr_{1.5}Co_{0.5}O_{8-\delta}$ was synthesized by a pseudo sol–gel method, based on the thermal decomposition of propionate precursors [13]. The starting materials for Ce, Zr and Co were cerium(III) acetate hydrate, zirconium(IV) acetylacetonate and cobalt(II) acetate hydrate, which all led exclusively to propionate precursors in propionic acid. The starting salts were dissolved in boiling propionic acid in a concentration of 0.12 mol L^{-1} in cation. The three boiling solutions were mixed and the solvent was evaporated until a resin was obtained. The resin was heating at 2 °C min^{-1} under air until 500 °C and maintained 6 h at this temperature.

The crystallinity of the Ce-Zr-Co mixed oxide was studied by X-ray diffraction (Siemens D5000, Cu Kα radiation, $20^\circ < 2\theta < 65^\circ$, 0.06° min^{-1}).

The micro-homogeneity of the catalyst and the carbon deposit were studied by TEM-EDXS analyses on a TOPCON EM-002B apparatus (acceleration voltage 200 kV).

The reducibility was studied by TPR. The TPR measurements were carried out on 50 mg of catalyst heated from room temperature to 900 °C at 15 °C min^{-1} under 10% H_2/He with a total gas flow of 50 mL min^{-1}.

To characterize the ''activated'' catalysts (catalysts after partial reduction at 440 °C), TPR of reduced catalysts have been performed. After in situ reduction, inert gas was admitted on the catalyst and temperature was decreased to room temperature. Then, classical TPR was performed and compared to that of the unreduced catalyst.

The morphology of the catalyst after test was studied by SEM on a JEOL JSM-6700F apparatus.

Carbon deposit produced during steam reforming was analyzed by TPO: aged sample (25 mg) is heated from room temperature to 900 °C at 15 °C min^{-1} under a 5% O_2/He mixture.

2.3. Catalytic tests

The ethanol steam reforming reaction was carried out in a fixed bed reactor, at atmospheric pressure.

The $Ce_2Zr_{1.5}Co_{0.5}O_{8-\delta}$ catalyst (0.16 g) was first submitted to in situ reduction under a pure hydrogen flow (3 mL min^{-1}), heated at 2 °C min^{-1} from room temperature to 440 °C, maintained 12 h at 440 °C. After reduction, the

H_2 flow was stopped and an Ar:N_2 mixture (2.1 L h^{-1}; 4:1 M) was introduced in the reactor to remove hydrogen. The temperature was increased to the reaction temperature of 540 °C. The reaction mixture ethanol:water (1:6 M; 0.9 L h^{-1} gas) or real bioethanol solution mixture (ethanol:-water 1:5.95 M; 0.9 L h^{-1} gas) was then introduced (GHSV = 26,000 h^{-1}).

The gas products were analyzed on-line by micro-gas chromatography.

The reactivity test procedure was identical to study real bioethanol steam reforming.

The results are expressed in terms of molar selectivity in the gas phase for H_2, CO_2, CO, CH_3CHO, C_2H_4, CH_4 and CH_3COCH_3. When considering only the steam reforming reaction ($C_2H_5OH + 6H_2O \rightarrow 6H_2 + 2CO_2$), a maximum of 75% can then be obtained for the hydrogen selectivity in our reaction conditions.

The hydrogen yields are expressed in gram of hydrogen per hour per gram of catalyst, the maximum H_2 yield which can be obtained in our reaction conditions is of 0.45 $gH_2\ h^{-1}\ g_{cat}{}^{-1}$.

3. Results and discussion

3.1. Characterization before test

In Fig. 1 are presented the diffractograms of the $Ce_2Zr_{1.5}Co_{0.5}O_{8-\delta}$ mixed oxide, after ethanol steam reforming and after bioethanol steam reforming (a), (b) and (c), respectively.

The preparation method allows the crystallization of the mixed oxide without any phase rejection. No single oxide is detected (CeO_2, ZrO_2, Co_3O_4) but only one cubic structure corresponding to the $Ce_2Zr_2O_8$ fluorite (Fig. 1a). Cobalt is then either inserted in the fluorite lattice or dispersed under the form of very small oxide particles.

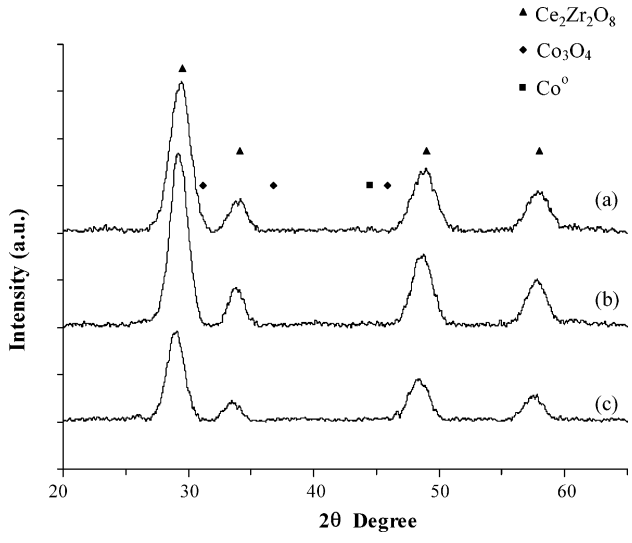

Fig. 1. Diffractograms of $Ce_2Zr_{1.5}Co_{0.5}O_{8-\delta}$: (a) fresh; (b) after ethanol reforming; (c) after bioethanol reforming.

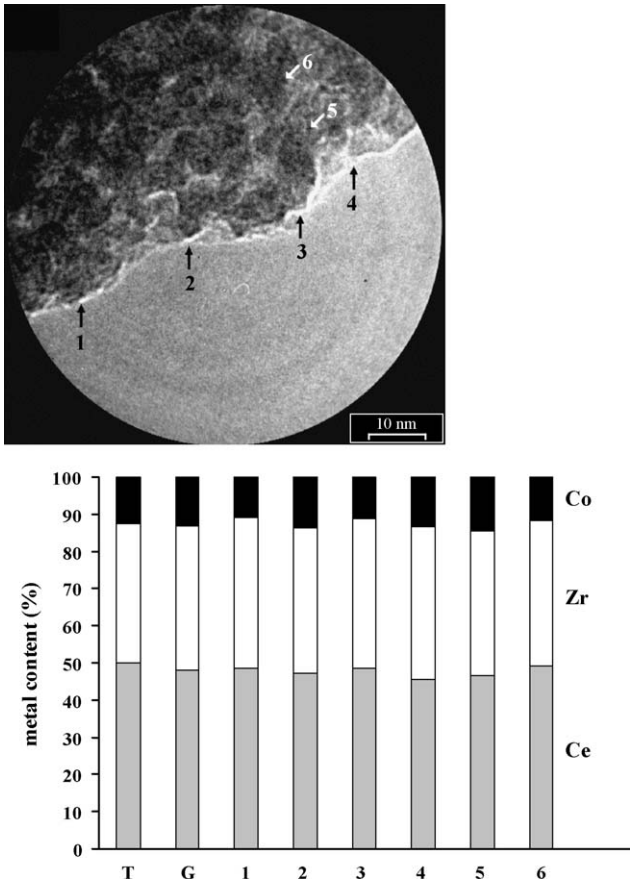

Fig. 2. TEM micrograph of the fresh catalyst and corresponding micro-analyses. T: theoretical value; G: 200 nm probe; 1–6: 14 nm probe.

The fresh catalyst has been observed by TEM. Elemental micro-analysis has been performed with probes of various sizes: 200 and 14.4 nm. The results are presented in Fig. 2.

The size distribution is monodisperse (5–10 nm), the particles are well crystallized.

The micro-homogeneity of the catalyst has been controlled by EDXS micro-analysis. The global elemental composition (200 nm probe) of the fresh oxide is near to the theoretical value expected for $Ce_2Zr_{1.5}Co_{0.5}O_{8-\delta}$: 48.0% of Ce; 38.9% of Zr; 13.1% of Co instead of respectively, 50; 37.5 and 12.5%.

The results of analyses performed on different areas of the samples with the 14.4 nm probe (results 1–6 in Fig. 2) are comparable. The local cerium; zirconium and cobalt contents vary respectively between 45.5 and 48.3%; 38.8 and 40.6%, and 10.9 and 14.5%. This accounts for the high micro-homogeneity of the fresh catalyst.

All the characterizations are in favor of cobalt insertion in the fluorite lattice rather than rejection of small cobalt oxide crystallites which would result in different compositions in different areas of the sample. The formation of mixed propionates during the polymerization step of the preparation would pre-form the Co–O–Zr or Co–O–Ce bonds as well as Zr–O–Ce bonds, and ensure the insertion of cobalt in the mixed oxide lattice.

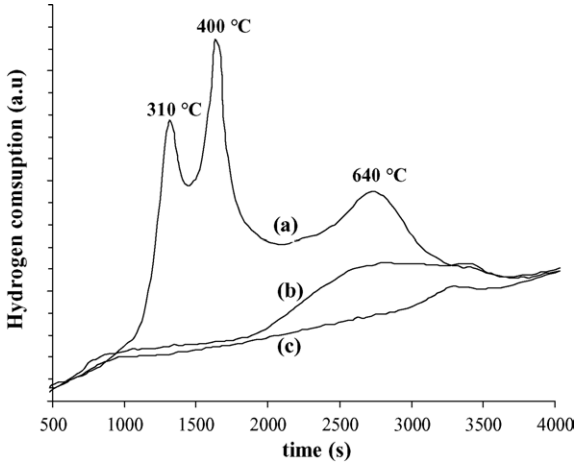

Fig. 3. TPR profiles of $Ce_2Zr_{1.5}Co_{0.5}O_{8-\delta}$: (a) fresh; (b) after slow reduction at 440 °C; (c) after reduction at 750 °C.

The $Ce_2Zr_{1.5}Co_{0.5}O_{8-\delta}$ being prepared to be then reduced to generate metal cobalt particles, attention has been paid to its reducibility. First, its hydrogen consumption versus temperature was followed by TPR. The TPR profile is presented in Fig. 3a.

The reduction proceeds in three steps at 310, 400 and 640 °C. As a comparison, the TPR behavior of a cobalt free $Ce_2Zr_2O_8$ was studied. For this oxide the reduction of Ce^{4+} into Ce^{3+} occurs at 450 °C. Assuming that insertion of cobalt instead of zirconium in the mixed oxide does not affect much the reduction temperature of cerium, the other reduction steps (310 and 640 °C) can be ascribed to cobalt reduction. A previous work [15] specifically dedicated to the reduction process of the Ce-Zr-Co oxides by means of magnetic measurements showed that at 440 °C 75% of cobalt of the sample is reduced into Co°, the complete reduction of cobalt into Co° being achieved at 640 °C.

To favor the metal-oxide interactions which seem to be the key point for the catalysts stability under test, the $Ce_2Zr_{1.5}Co_{0.5}O_{8-\delta}$ was only partially reduced according to the following procedure: in situ reduction under a pure H_2 flow (3 ml min^{-1}), heated at 2 °C min^{-1} from room temperature to 440 °C, maintained 12 h at 440 °C.

To characterize the ''partially reduced'' catalyst, TPR of reduced catalyst has been performed. The catalyst was first reduced according to the reduction procedure described before, inert gas was then admitted on the catalyst and temperature was decreased to room temperature. Then, classical TPR was performed and compared to that of the unreduced catalyst. The TPR profile of the ''partially reduced'' catalyst is given in Fig. 3b. For comparison, the TPR profile of the totally reduced catalyst (pure H_2 flow at 750 °C) is given in Fig. 3c.

It clearly appears that the two first reduction steps at 310 and 400 °C have disappeared for the reduced samples. The reduction at 750 °C is efficient to reduce totally the catalyst. In that case (Fig. 3c) the hydrogen consumption is negligible (0.04 mL of H_2 compared to 2.32 mL for the fresh catalyst). That is to say that the high temperature reduction of the catalyst consists in the total reduction of cobalt into Co° and in the partial reduction of Ce^{4+} into Ce^{3+}.

The slow reduction at 440 °C is not total. After slow reduction (Fig. 3b), the catalysts still consumes 0.48 mL of H_2 at high temperature. In that case a maximum of 75% of cobalt is reduced into Co°. The partial reduction state is stable under reducing atmosphere at 440 °C.

3.2. Catalytic results

The evolution of the catalytic behavior with time on stream is given in Figs. 4–6. In Fig. 4a are given the ethanol conversion and the molar product distribution of the main products (H_2, CO_2 and CO) in the gas phase for the reaction with the ethanol/water mixture. The results of the catalytic test with bioethanol solution are given in Fig. 4b.

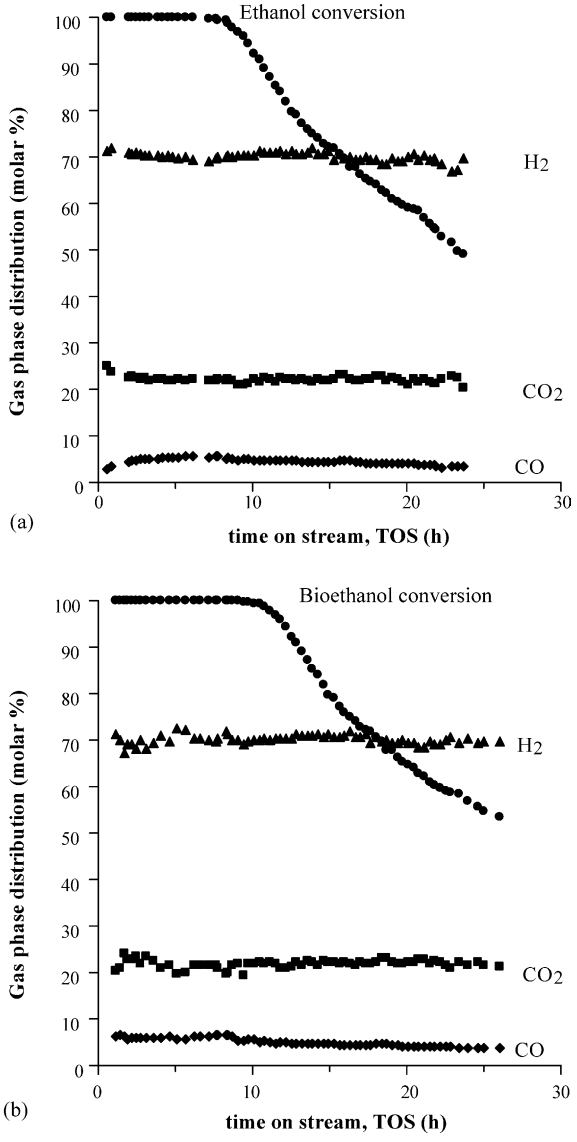

Fig. 4. Ethanol conversion and molar distribution of H_2, CO_2 and CO in the gas phase of (a) water/ethanol mixture and (b) bioethanol solution.

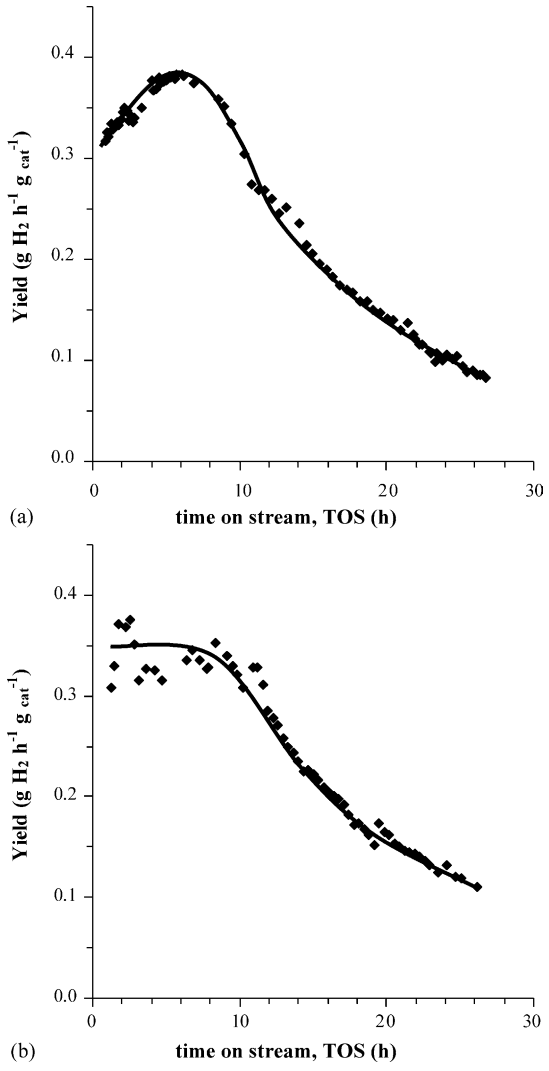

Fig. 5. Hydrogen yield in the steam reforming reaction of (a) water/ethanol mixture and (b) bioethanol solution.

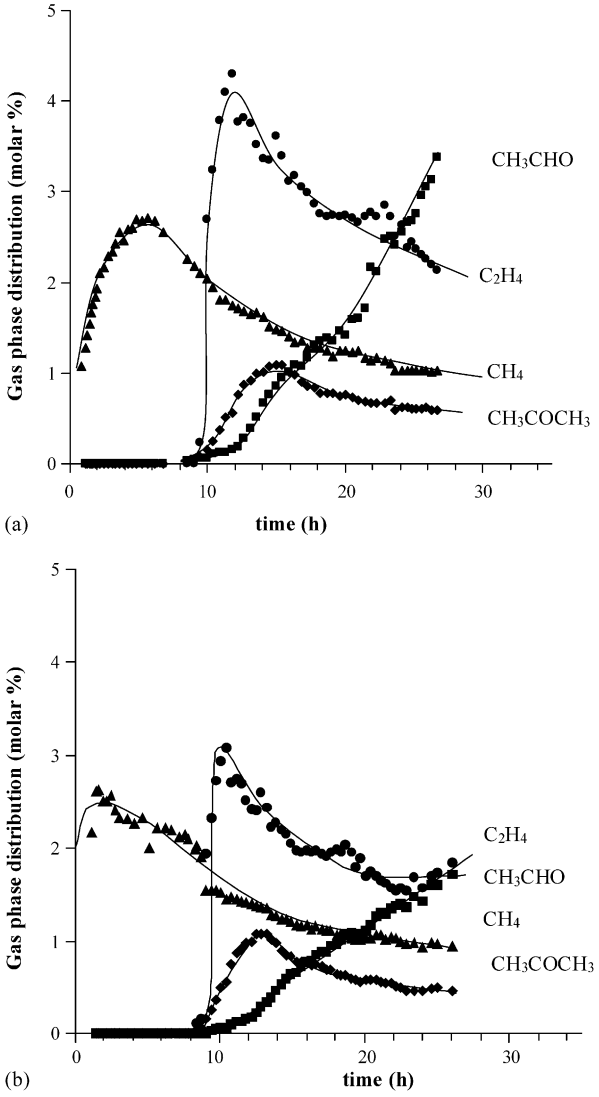

Fig. 6. Gas phase distribution (molar) of CH_4, C_2H_4, CH_3CHO and CH_3COCH_3 in the gas phase (a) water/ethanol mixture and (b) bioethanol solution.

For the bioethanol steam reforming reaction, the ethanol conversion is total (100%) during the first 11 h of test. During that period of time the molar distribution of the main products in the gas phase is stable: 70.1% of H_2, 21.4% of CO_2 and 6.4% of CO. After 11 h of reaction, the ethanol conversion begins to decline and is only 55% after 24 h and 53% after 26 h of test. The molar distribution of the main products in the gas phase is almost unchanged except for CO: 69.8% of H_2, 21.4% of CO_2, 3.9% of CO. We can note that the CO selectivity is strongly decreased (60% less CO than in the first hours of reaction).

For the ethanol/water mixture (Fig. 4a), the catalytic behavior is similar. The ethanol conversion is first total, but begins to decline after 9 h, earlier than with the bioethanol solution. After 26 h of reaction the ethanol conversion is only 44% (compared to 53% in the case of bioethanol). The variation of the gas phase distribution is similar and the molar distribution of the main products after 26 h of test is: 68.4% of H_2, 21% of CO_2 and 3.1% of CO.

The hydrogen yield is given in Fig. 5.

For bioethanol reforming, the hydrogen yield (Fig. 5b) varies between 0.35 and 0.38 g H_2 h^{-1} $g_{cat}{}^{-1}$ during the first 11 h of reaction. Then it decreases gradually to 0.11 g H_2 h^{-1} $g_{cat}{}^{-1}$. This decrease is more a consequence of the loss of activity of the catalyst (lower ethanol conversion) than of the selectivity variations with time, since the H_2 selectivity only slightly decreases with time (see Fig. 4b).

For the ethanol/water mixture (Fig. 5a), the evolution is similar but the hydrogen production is always slightly lower than in the case of bioethanol. The decrease of the H_2 yield begins earlier than for bioethanol, in accordance with the earliest decline of ethanol conversion discussed before. After 26 h, the H_2 yield is 0.09 g H_2 h^{-1} $g_{cat}{}^{-1}$.

The better H_2 yields obtained from bioethanol could be explained by the steam reforming of other alcohols (methanol, *n*-propanol, *n*-butanol and *iso*-amilic alcohol)

present in the solution after distillation, in addition to ethanol (on which is based the overall carbon balance).

To understand the deactivation process of the catalyst under test, attention was paid to the evolution of the byproducts formation with time on stream. In Fig. 6 ((a) for the ethanol/water mixture and (b) for bioethanol solution) are given the molar distribution in the gas phase of methane, ethylene, acetaldehyde and acetone.

Among these byproducts, only CH_4 is detected in the first hours of reaction. Comparing the two respective curves, the CH_4 production seems to be closely related to the H_2 production. We can consider that CH_4 is produced starting from hydrogen by reaction with either ethanol according to: $C_2H_5OH + H_2 \rightarrow 2CH_4 + H_2O$ or by reaction with CO according to: $CO + 2H_2 \rightarrow CH_4 + H_2O$, being then closely linked to the hydrogen production.

In the case of bioethanol reforming, just before the decline of ethanol conversion after 11 h of test, other undesirable products begin to appear. The first byproduct detected is acetone (∼8:15 h), then ethylene (∼8:45 h) and finally acetaldehyde (∼9:30 h). After 26 h of test, the gas phase contains 0.9% of CH_4, 1.8% of C_2H_4, 1.7% of CH_3CHO and 0.5% of CH_3COCH_3.

For the ethanol/water mixture reforming, the profile of the curves is similar. We can just note the much higher production of acetaldehyde in that case. After 26 h of test, the gas phase contains 1.0% of CH_4, 2.7% of C_2H_4, 3.1% of CH_3CHO and 0.6% of CH_3COCH_3.

3.3. Characterization after test

After catalytic test (with ethanol or bioethanol) the diffractograms (Fig. 1b and c, respectively) are very similar to that of the fresh catalyst. Once more, only the cubic fluorite structure is detected. The structure is preserved after 26 h of reactivity test and no metallic Co° is observed. However, it has to be noted that the diffraction peaks of the catalysts after test are shifted towards the smaller diffraction angles. That indicates an enlargement of the lattice, in agreement with the reduction of the oxide.

The catalyst was studied by TEM after bioethanol reaction. The results of microanalysis probes are presented in Fig. 7.

After catalytic test the global composition of the catalyst (analysis with the 200 nm probe) has changed. The three global analyses vary between 23 and 48% for Ce, 29 and 37% for Zr and 15 and 47% for Co. The changes are more noticeable with the 12 local analyses (with the 8.8 nm probe). The local Co content varies between 8 and 95%. Some areas correspond to almost pure cobalt grains

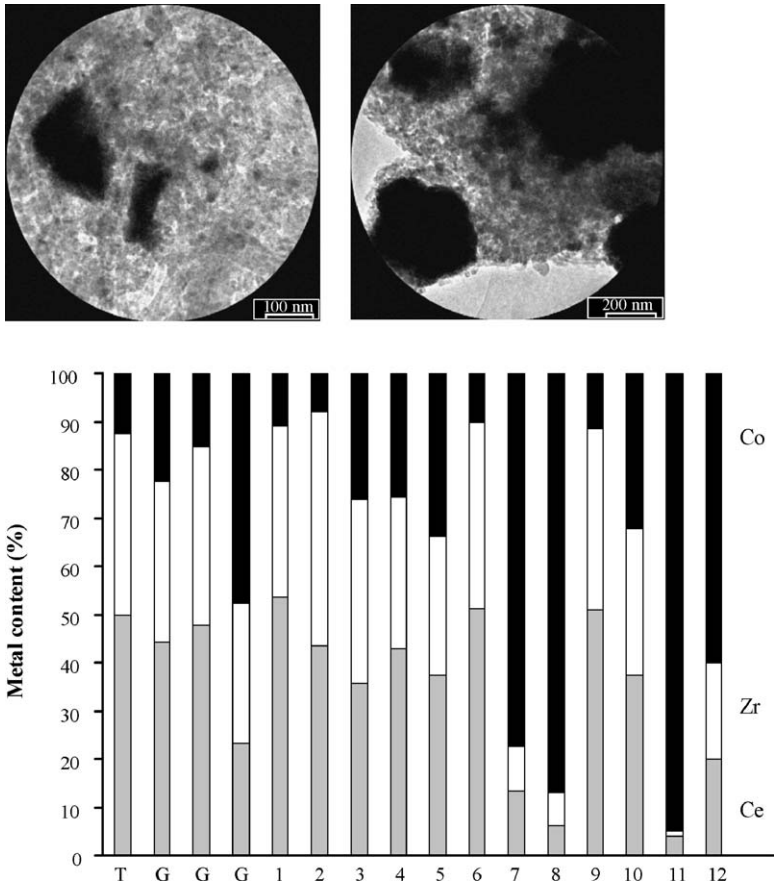

Fig. 7. TEM micrograph of the catalyst after bioethanol reforming and corresponding microanalyses. T: theoretical value; G: 200 nm probe; 1–12: 8.8 nm probe.

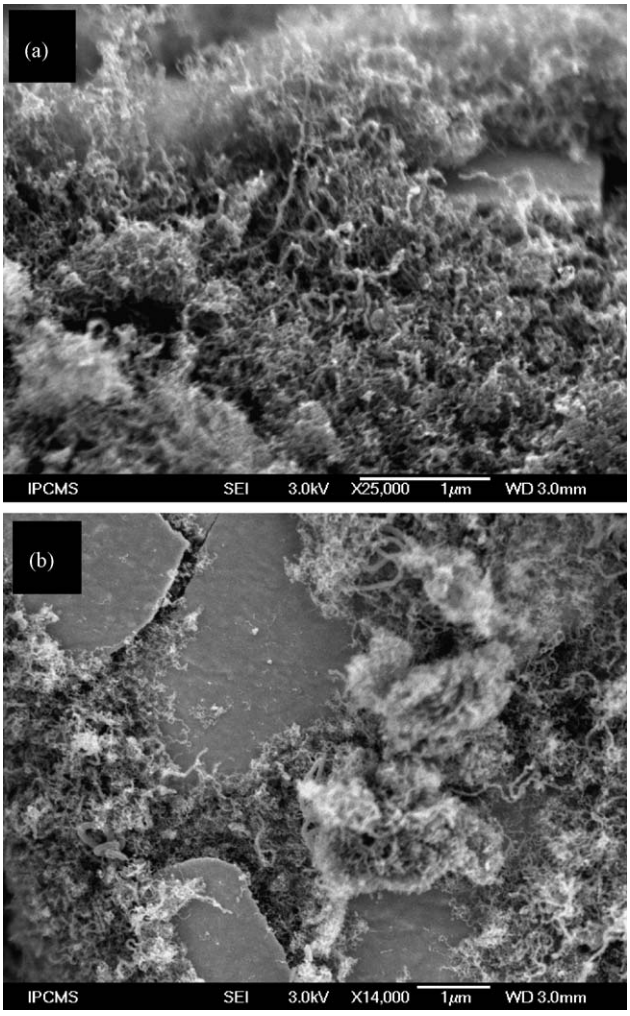

Fig. 8. SEM micrographs of the catalyst after reforming (a) ethanol/water mixture and (b) bioethanol solution.

(analyses 7, 8 and 11). The decrease of the local cobalt content in other areas (analyses 1, 2, 6 and 9) may be due to the reduction process which reduces part of cobalt of the oxide structure into metallic cobalt particles on a still cobalt-containing Ce-Zr-Co oxide [15].

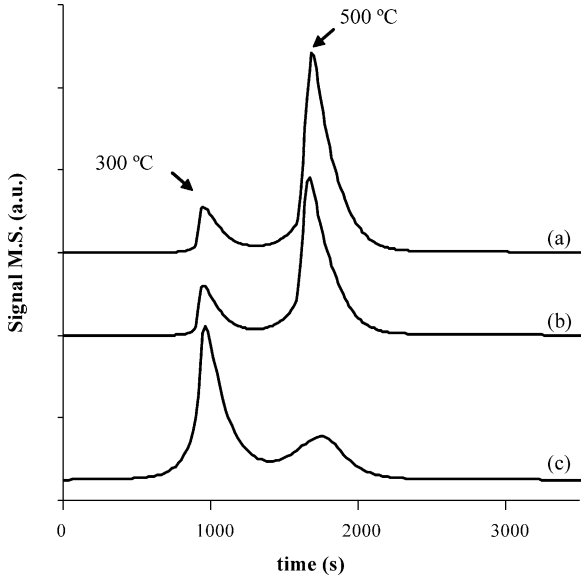

Fig. 10. TPO profiles of the catalyst after reforming of; (a) ethanol/water mixture at 540 °C; (b) bioethanol solution at 540 °C; (c) bioethanol solution at 440 °C.

The formation of carbon deposit on the catalyst under the reaction conditions was evidenced by SEM observations. In Fig. 8 are presented the micrographs of the catalyst after ethanol/water mixture reforming (Fig. 8a) and after bioethanol solution reforming (Fig. 8b). Carbon filaments clearly appear in the two cases on the surface of the grains.

TEM observations after test reveal two types of carbon species (see Fig. 9): either carbonaceous layers on the surface of the grains (Fig. 9a), either filaments (Fig. 9b) as evidenced by SEM.

The formation of two types of carbon deposits is confirmed by TPO experiments (Fig. 10). The TPO profiles of the catalyst after ethanol/water mixture reforming at 540 °C (Fig. 10a) and after bioethanol reforming at 540 °C (Fig. 10b) are very similar. They present two peaks at 300 and 500 °C which can be ascribed respectively to carbonaceous species and carbon filaments. The respective surfaces of the two peaks indicate that in both cases, carbon

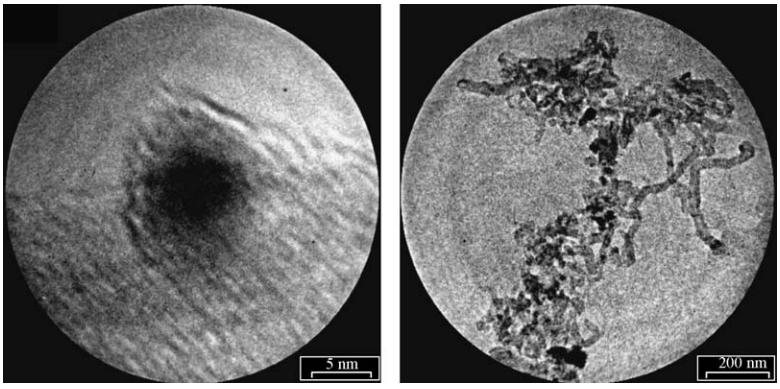

Fig. 9. TEM micrographs of the catalyst after bioethanol reforming.

filaments deposit is favored compared to carbonaceous species formation.

The change of the catalytic behavior with time on stream can be related with the time during which the oxide is in contact with the reducing atmosphere after the in situ reduction. After reduction at 440 °C, part of cobalt is reduced and the catalyst is then composed on small Co° particles in strong interaction with a Ce-Zr-Co oxide. This partially reduced catalyst is stable under reducing atmosphere at 440 °C, that is to say that total cobalt reduction is not achieved under these conditions [15].

The catalytic results presented here are obtained at 540 °C. At this temperature, and due to the high H_2 production, the catalyst undergoes deeper reduction under test. The decreasing cobalt content in the oxide support weakens the metal/support interaction and the metal stability under reaction conditions. Carbon deposition begins to occur and deactivates the catalyst. During the catalytic test, the formation of carbon filaments on metal particles separates the cobalt particles from the oxide support and then decreases again its stability.

The catalytic behavior with time presented here is typical of catalyst deactivation due to carbon deposition, as reported by Goula et al. [9].

When bioethanol reforming is performed at 440 °C (temperature under which the partially reduced catalyst is stable even under reducing conditions), the catalytic stability is much higher.

The bioethanol conversion versus time on stream is given in Fig. 11 when reforming is performed at 440 and at 540 °C. For a reaction temperature of 440 °C, the ethanol conversion is total (100%) in the first hours of reaction. After 26 h, the ethanol conversion is 90% (compared to 44% after 26 h at 540 °C). After 80 h under test, the catalyst still converts 60% of ethanol at 440 °C.

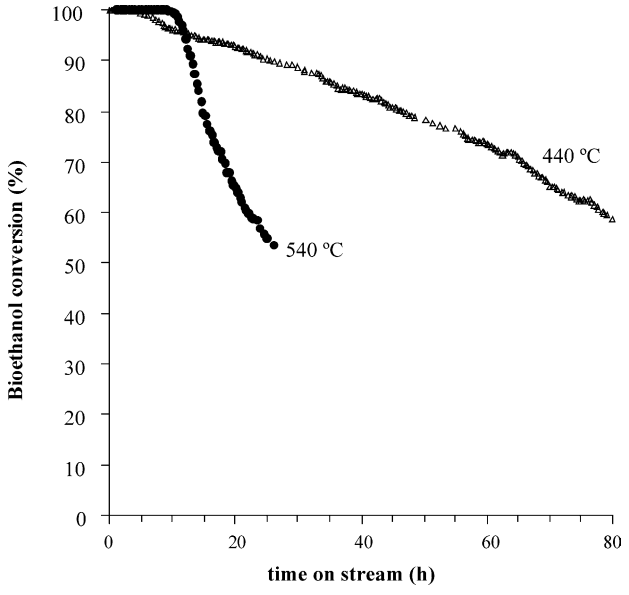

Fig. 11. Ethanol conversion versus time at 540 and 440 °C.

In Fig. 11c is given the TPO profile of the catalyst after bioethanol reforming at 440 °C. The two peaks accounting for the two carbon types are still present but it clearly appears that their relative intensity is changed. At 440 °C, contrary to what occurred at 540 °C, carbonaceous species formation is largely favored compared to carbon filaments deposit.

In that case, the stabilization of cobalt metal particle by the cobalt-containing oxide is the key point to prevent the carbon deposition under the form of filaments and the subsequent deactivation.

4. Conclusion

The preparation method based on propionates polymerization in solution allows the cobalt integration in the fluorite lattice to obtain a mixed oxide of formula $Ce_2Zr_{1.5}Co_{0.5}O_{8-\delta}$, with high micro-homogeneity, as confirmed by XRD and TEM-EDXS analyses.

The Co°/Ce-Zr-Co oxide catalyst, obtained after partial in situ reduction, is efficient to convert ethanol into hydrogen with high selectivity. The catalytic behaviors are similar when using a water/ethanol mixture or a bioethanol solution (ethanol, water, methanol, higher alcohols). But slightly better results are obtained with bioethanol reforming.

The in situ controlled partial reduction (440 °C) of part of cobalt of $Ce_2Zr_{1.5}Co_{0.5}O_{8-\delta}$ generates nano-particles of Co° in strong interaction with the still cobalt-containing support they come from. Under the reaction conditions (540 °C, high H_2 production), the partially reduced catalyst undergoes deeper reduction. Cobalt cations of the oxide support begin to reduce, weakening metal-support interactions and carbon deposition, mainly carbon filaments, slowly deactivate the catalysts.

When the reforming of bioethanol is performed at 440 °C (temperature under which the partially reduced catalyst is stable even under reducing conditions), the deactivation is clearly checked. In that case, the carbon deposition mainly leads to carbonaceous species which do not induce so much deactivation than carbon filaments.

Acknowledgments

The authors thank the ECOS – Nord program n° C03P04, COLCIENCIAS/ICETEX/ICFES (Colombia) and the French Embassy in Colombia, for financial support.

References

[1] H.L. Chum, R.P. Overend, Fuel Process. Technol. 71 (2001) 187.
[2] J. Llorca, P. Ramírez de la Piscina, J. Sales, N. Homs, Chem. Commun. (2001) 641.

[3] A.N. Fatsikostas, D.I. Kondarides, X.E. Verykios, Catal. Today 75 (2002) 145.
[4] J. Llorca, N. Homs, J. Sales, P. Ramírez de la Piscina, J. Catal. 209 (2002) 306.
[5] J. Llorca, J.A. Dalmon, P. Ramírez de la Piscina, N. Homs, Appl. Catal. A 243 (2003) 261.
[6] F. Mariño, G. Baronetti, M. Jobbagy, M. Laborde, Appl. Catal. A 238 (2002) 41.
[7] M.S. Batista, R.K.S. Santos, E.M. Assaf, J.M. Assaf, E.A. Ticianelli, J. Power Sources 124 (2003) 99.
[8] J.P. Breen, R. Burch, H.M. Coleman, Appl. Catal. B 39 (2002) 26.
[9] M.A. Goula, S.K. Kontou, P.E. Tsiakaras, Appl. Catal. B 49 (2004) 135.
[10] J. Llorca, P. Ramírez de la Piscina, J.A. Dalmon, J. Sales, N. Homs, Appl. Catal. B 43 (2003) 355.
[11] J. Comas, F. Mariño, M. Laborde, N. Amadeo, Chem. Eng. J. 98 (2004) 61.
[12] N. Kosaric, F. Vardar-Sukan, in: M. Roehr (Ed.), The Biotechnology of Ethanol. Classical and Future Applications, Wiley-VCH, Weinheim, 2001 , p. 182 (Part II, Chapter 6).
[13] J.C. Vargas, F. Sternenberg, A.C. Roger, A. Kiennemann, Chem. Eng. Trans. 4 (2004) 262.
[14] J.C. Vargas, E. Vanhaecke, A.C. Roger, A. Kiennemann, Stud. Surf. Sci. Catal. 147 (2004) 115.
[15] A.C. Roger, E. Vanhaecke, J.C. Vargas, A. Kiennemann, in: Proceedings of the European Hydrogen Energy Conference EHEC, Grenoble (France) 2–5 September, 2003.